

Abstract: Thousands of exoplanets have been detected, but only one exoplanetary transit was potentially observed in X-rays from HD 189733A. What makes the detection of exoplanets so difficult in this band? Using Monte-Carlo radiative transfer simulations, we compute the amount of X-ray coronal flux reprocessed by the extended evaporating-atmosphere of HD 189733b. In the 0.25–2 keV energy band, the maximum depth of the XMM-Newton light curve is about 1.6% at 47 min apart from the transit center on the geometrically thick and optically thin corona, and little sensitive to the metal abundance (assuming that adding metals in the atmosphere would not dramatically change the density-temperature profile). Regarding a direct detection of HD 189733b in X-rays, we find that the amount of flux reprocessed by the exoplanetary atmosphere from egress to transit decays from 3 to 5 orders of magnitude fainter than the flux of the host star. Additionally, the degree of diluted linear polarization emerging from HD 189733A is lower than 0.003%, and largest near planetary greatest elongations. This implies that neither the modulation of the X-ray reprocessed flux with the orbital phase nor the scattered-induced continuum polarization can be observed with current X-ray facilities.

1. The HD 189733 system

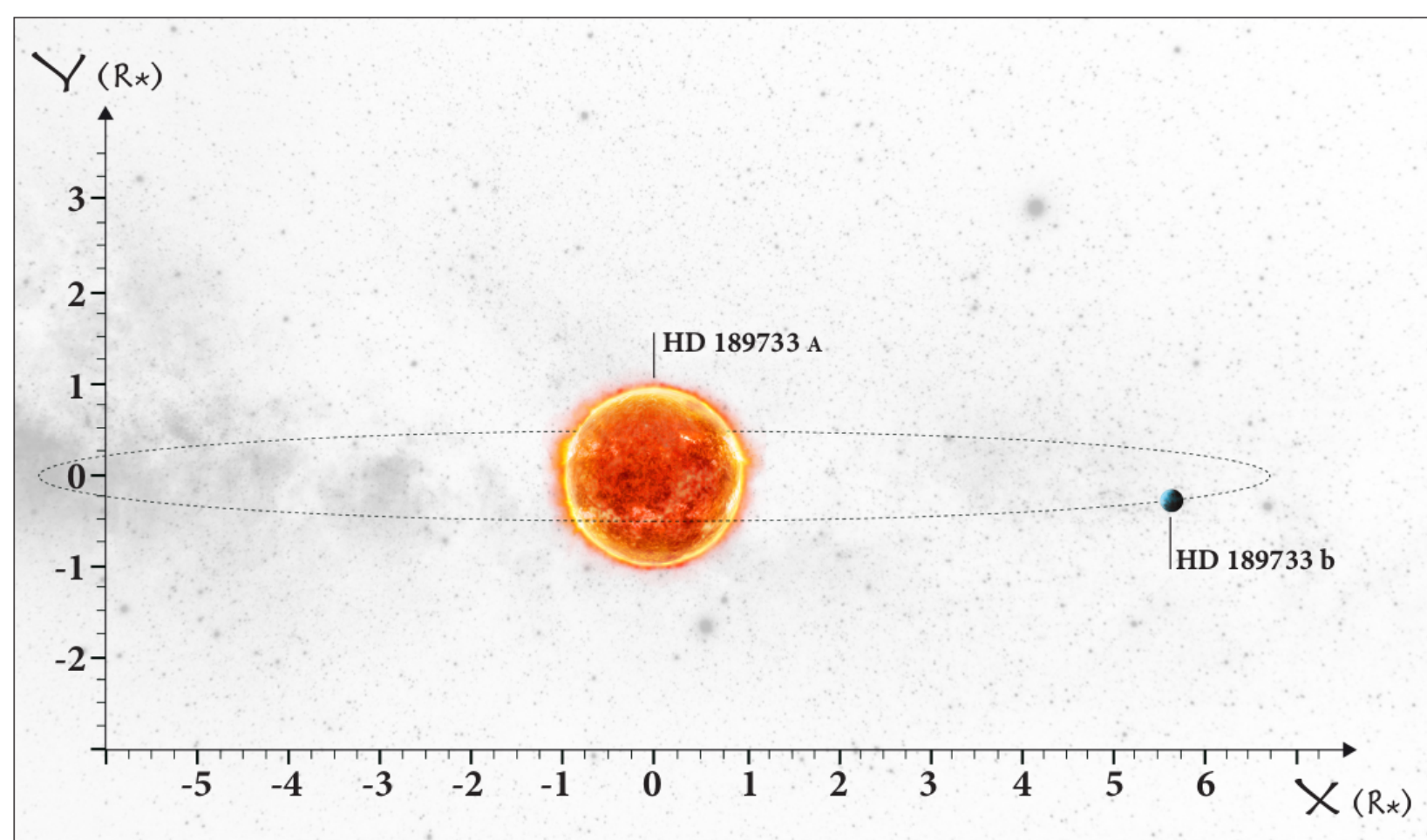


Figure 1 : Artist representation of the system. Note the limb brightening of the geometrically thick, optically thin, stellar corona.

The exoplanet HD 189733b with mass $1.162 M_J$ (de Kok et al. 2013) and radius $1.26 R_J$, was discovered by transit observations in optical (Bouchy et al. 2005). Orbiting around HD 189733A in 2.219 days (Triaud et al. 2009), this Hot Jupiter is situated at only 0.031 au from its host star. With its X-ray flux of $\sim 3 \times 10^{-13} \text{ erg cm}^{-2} \text{ s}^{-1}$ in the 0.25–2 keV band, corresponding to a luminosity of $\sim 10^{28} \text{ erg s}^{-1}$ and $L_X/L_{\text{bol}} \sim 10^{-5}$, HD 189733A was a perfect target for tentative detection of X-ray exoplanetary transits (Poppenhaeger et al. 2013) and radiative transfer simulations in X-rays reported here.

2. Model of the HD 189733A quiescent corona

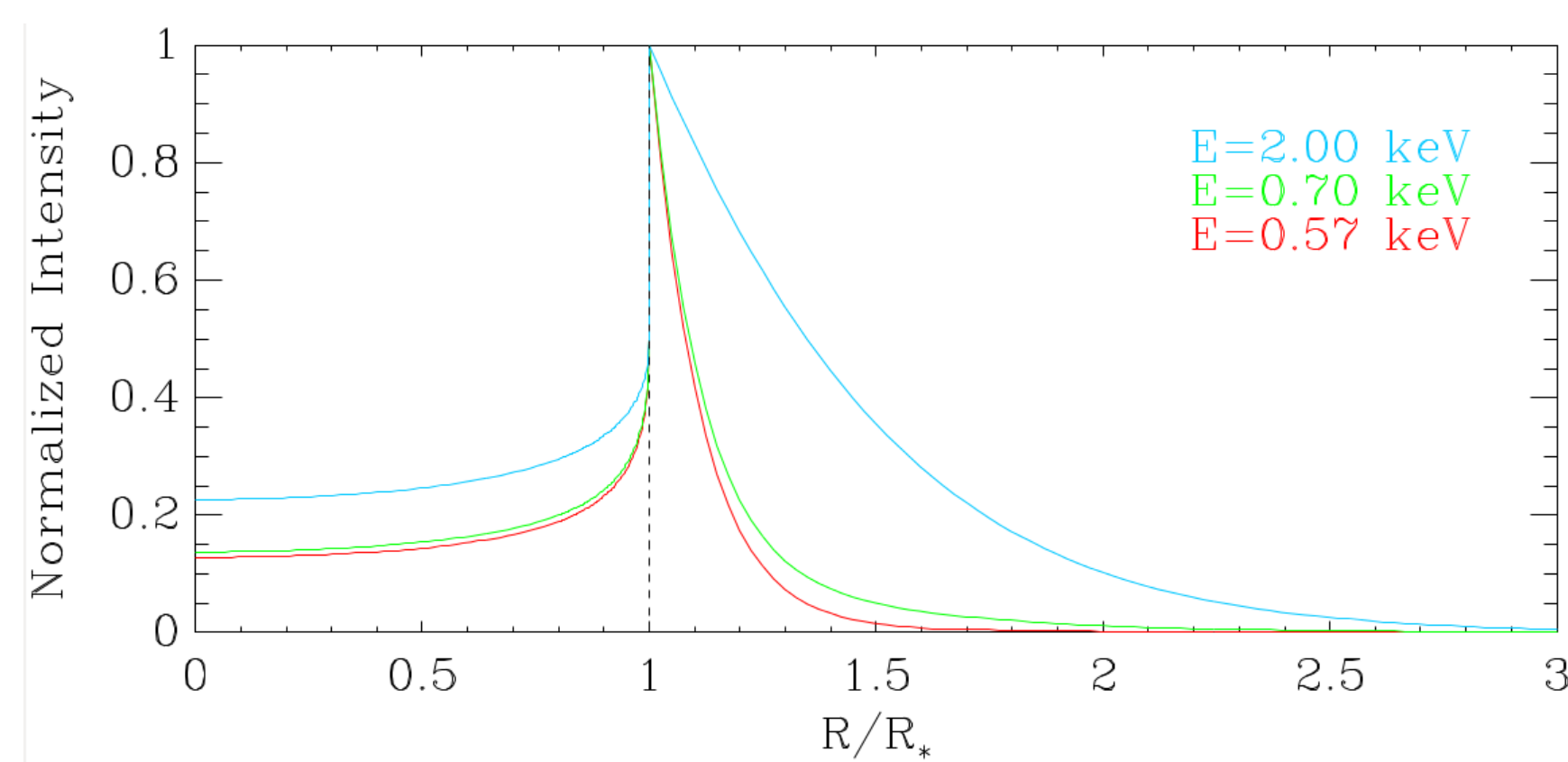


Figure 2 : Coronal emission profile integrated along the line of sight versus the distance from the stellar center. All the profiles have been normalized at the stellar limb (vertical dashed line). The green line is the coronal emission profile at 0.7 keV (the mean energy of the photons detected in the 0.25–2 keV energy band by XMM-Newton pn) that we used in our simulation.

In our model, we define the quiescent corona has layers of constant, isotropic, and optically thin emission, above an optically thick sphere of radius R_* corresponding to the stellar photosphere. Since ordinary bremsstrahlung emission from plasma shows no intrinsic polarization due to the random motions of electrons, we consider only unpolarized X-ray photons from the stellar corona.

3. Model of the HD 189733b atmosphere

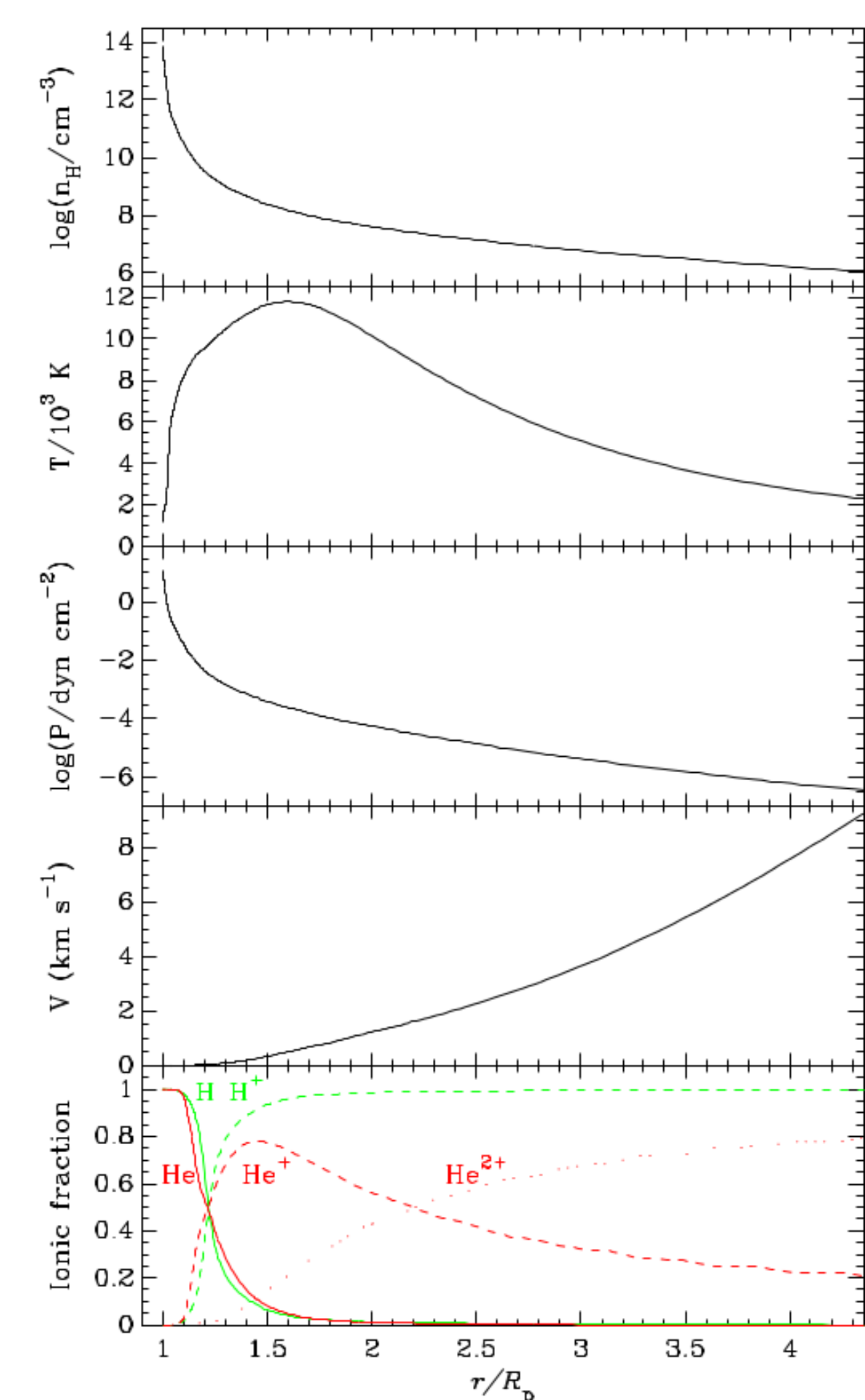


Figure 3 : Atmospheric model of HD 189733b of Salz et al. (2015) used in our X-ray simulation.

The physical properties of the upper atmosphere of HD 189733b can be constrained with transmission spectroscopy of HD 189733A (e.g., Lecavelier Des Etangs et al. 2008). The gas of the HD 189733b atmosphere is photoionized by the UV emission of HD 189733A (e.g., Sanz-Forcada et al. 2011) and cools by radiation from collisionally excited atomic hydrogen, which leads similarly to H II regions to a temperature of about 10000 K. This high temperature produces a (slow) evaporative-wind (Yelle 2004; Murray-Clay et al. 2009).

Salz et al. (2015) obtained a 1D, spherically symmetric hydrodynamic simulations of the escaping atmosphere of HD 189733b, predicting gas velocity of $\sim 9 \text{ km s}^{-1}$ at the Roche's radius (4.35 times the planetary radius) by coupling a detailed photoionization and plasma simulation code with a general MHD code, and assuming only atomic Hydrogen and Helium in the atmosphere. Since the resulting temperature-pressure profile is consistent with the rise of temperature with the altitude observed by Huitson et al. (2012), we adopt the Salz et al. (2015)'s profiles to describe the thermosphere of HD 189733b.

4. X-ray light curves of the coronal transit

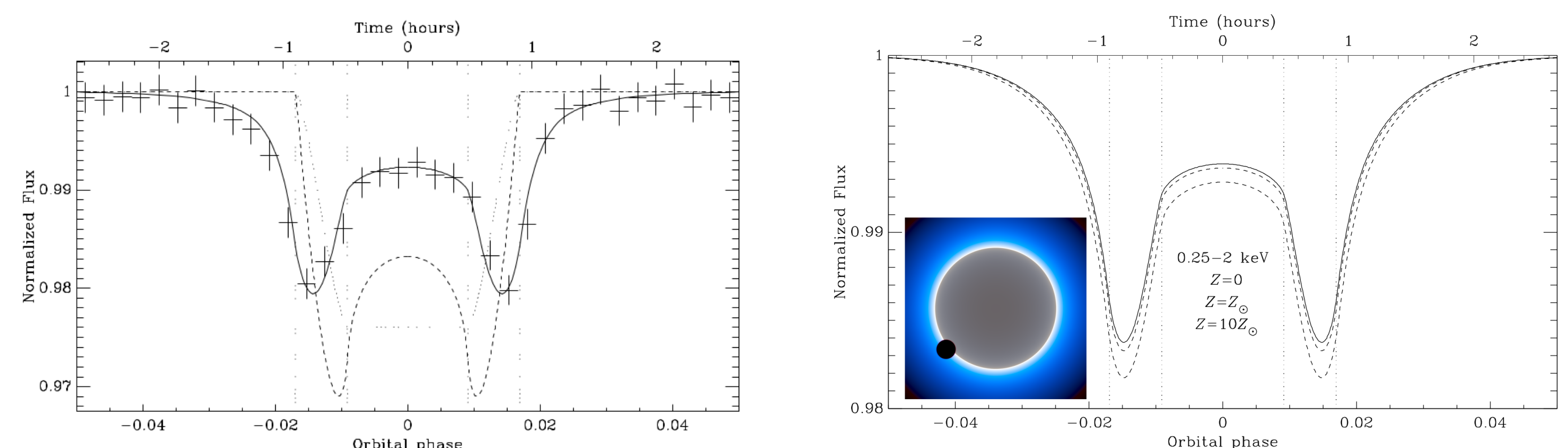


Figure 4 : Light curves of the planetary transits of HD 189733b. Left: the black solid line is the coronal transit at 0.7 keV computed for $R_X \sim 1.01 R_p$ (corresponding to a planetary atmosphere of H, He, and He^+). The cross data are the coronal transit signature obtained by our simulation. The dotted and dashed lines are the photospheric transit (see vertical dotted lines for 1st, 2nd, 3rd and 4th contacts) and the chromospheric transit (Schlawin et al. 2010) respectively. Right: weighted average coronal transit in the 0.25–2.0 keV energy band computed for XMM-Newton pn. The image (0.25–0.6, 0.6–0.8, 0.8–2 keV) shows the orbital phase where the transit depth is at maximum.

Despite its extended evaporating-atmosphere, we find that the X-ray absorption radius of HD 189733b at 0.7 keV is ~ 1.01 times the planetary radius for an atmosphere of atomic Hydrogen and Helium (including ions), and produces a maximum depth of $\sim 2.1\%$ at $\sim \pm 46$ min from the center of the planetary transit on the geometrically thick and optically thin corona. We compute numerically in the 0.25–2 keV energy band for XMM-Newton pn that this maximum depth is only of $\sim 1.6\%$ at $\sim \pm 47$ min from the transit center, and little sensitive to the metal abundance assuming that adding metals in the atmosphere would not dramatically change the density-temperature profile.

5. X-ray photo-polarimetry

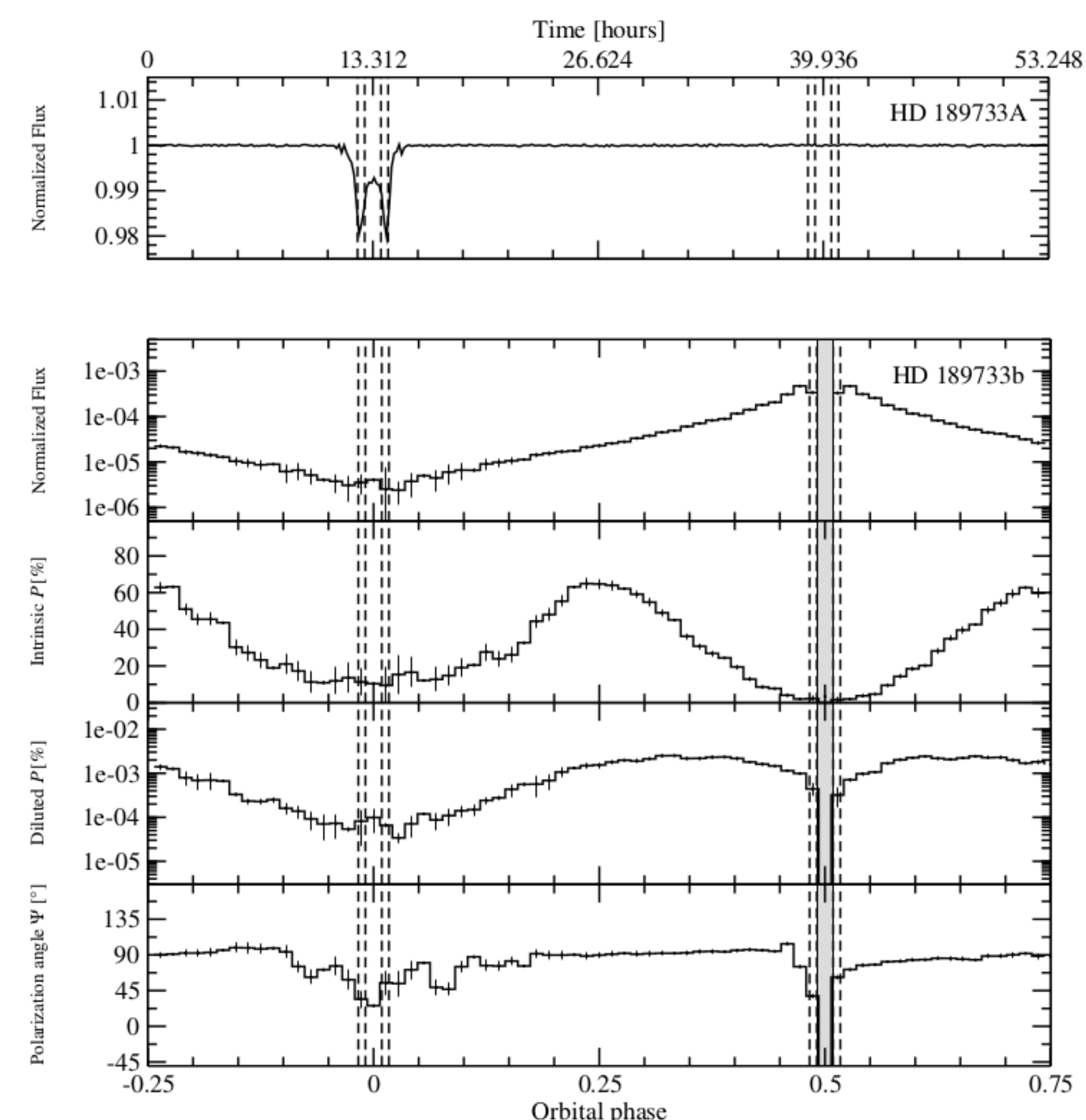


Figure 5 : Photometry at 0.7 keV of HD 189733A, and reprocessed flux from the surface of HD 189733b (first two panels). The fluxes are normalized to the initial flux of the star. Polarimetric results are shown in terms of P (polarization percentage) and ψ (polarization position angle, defined with respect to the vertical axis of the system). The error bars correspond to 1σ statistical errors in the Monte Carlo simulation. The gray box indicates a region where polarization measurement of HD 189733b is impossible due to the disappearance of the exoplanet behind its star.

To simulate the revolution of HD 189733b around its host star, we used the radiative transfer code STOKES (Goosmann & Gaskell 2007; Marin et al. 2012, 2015). We find that the exoplanet's flux is three to five orders of magnitude fainter than the host star's one, with maximums at egress and ingress points due to the asymmetrical scattering phase function of Compton and Rayleigh scattering. At most, the reprocessed flux is lower than $1.0 \times 10^{-16} \text{ erg cm}^{-2} \text{ s}^{-1}$. A detection of the flux modulation with orbital phase is in practical not achievable since requiring tremendous exposure time. The reprocessed flux is associated with a very weak, diluted, amount of linear polarization. The polarization degree being less than to 0.003%, it is impossible to measure it with the current technology of X-ray polarimeters.

6. Conclusions

Despite its extended evaporating-atmosphere, we find that the X-ray absorption radius of HD 189733b at 0.7 keV is ~ 1.01 times the planetary radius for an atmosphere of atomic Hydrogen and Helium (including ions), and produces a maximum depth of $\sim 2.1\%$ at $\sim \pm 46$ min from the center of the planetary transit on the geometrically thick and optically thin corona. In the 0.25–2 keV energy band observed with XMM-Newton pn, the predicted maximum depth is only of 1.6%.

Regarding a direct detection of HD 189733b in X-rays, we find both the modulation of the X-ray flux with the orbital phase and the scattered-induced continuum polarization cannot be observed with current X-ray facilities. However, the direct detection of the X-rays scattered by HD 189733b might be considered in the future with the possible advent of interferometric facilities in X-rays, e.g., the Black Hole Mapper visionary-mission with (sub)microarcsecond resolution (Kouveliotou et al. 2014).

These results were published in Marin & Grosso (2017, ApJ, 835, 283; arXiv:1701.00990).

